ECOHYDROLOGY
Ecohydrol. (2013)
DOI: 10.1002/eco.1394

The influence of vegetation on the hydrodynamics and geomorphology of a tree island in Everglades National Park (Florida, United States)

Pamela L. Sullivan,[1]* Vic Engel,[2] Michael S. Ross[1,3] and René M. Price[1,3]

[1] *Southeast Environmental Research Center, Florida International University, Miami, FL, USA*
[2] *Southeast Ecological Science Center, United States Geological Survey, Gainesville, FL, USA*
[3] *Department of Earth and the Environment, Florida International University, Miami, FL, USA*

ABSTRACT

Transpiration-driven nutrient accumulation has been identified as a potential mechanism governing the creation and maintenance of wetland vegetation patterning. This process may contribute to the formation of nutrient-rich tree islands within the expansive oligotrophic marshes of the Everglades (Florida, United States). This study presents hydrogeochemical data indicating that tree root water uptake is a primary driver of groundwater ion accumulation across one of these islands. Sap flow, soil moisture, water level, water chemistry, and rainfall were measured to identify the relationships between climate, transpiration, and groundwater uptake by phreatophytes and to examine the effect this uptake has on groundwater chemistry and mineral formation in three woody plant communities of differing elevations. During the dry season, trees relied more on groundwater for transpiration, which led to a depressed water table and the advective movement of groundwater and dissolved ions, including phosphorus, from the surrounding marsh towards the centre of the island. Ion exclusion during root water uptake led to elevated concentrations of all major dissolved ions in the tree island groundwater compared with the adjacent marsh. Groundwater was predominately supersaturated with respect to aragonite and calcite in the lower-elevation woody communities, indicating the potential for soil formation. Elevated groundwater phosphorous concentrations detected in the highest-elevation woody community were associated with the leaching of inorganic sediments (i.e. hydroxyapatite) in the vadose zone. Understanding the complex feedback mechanisms regulating plant/groundwater/surface water interactions, nutrient dynamics, and potential soil formation is necessary to manage and restore patterned wetlands such as the Everglades.

KEY WORDS ecohydrology; transpiration; phosphorus; ion accumulation; pedogenesis; groundwater/surface water interactions

Received 18 July 2012; Revised 16 April 2013; Accepted 18 April 2013

INTRODUCTION

Spatially varying transpiration rates are thought to cause anisotropic nutrient distributions and vegetation patterning across many landscape types (Heuperman, 1999; Rietkerk *et al.*, 2004; Engel *et al.*, 2005; Jackson *et al.*, 2009). In some wetlands, vegetation is characterized by a mosaic of slightly elevated hummocks or ridges of high-density vascular plants, surrounded by hollows containing a lower density of nonvascular vegetation (Rietkerk and van de Koppel, 2008). Positive feedbacks linking root water uptake to convergent fluxes of dissolved nutrients and increased plant growth have been cited as a formative factor in these wetlands and similarly structured habitats (Rietkerk *et al.*, 2004; Wetzel *et al.*, 2005; Ross *et al.*, 2006; Eppinga *et al.*, 2008; Saha *et al.*, 2010). In these systems, root uptake of groundwater during transpiration is thought to depress the water table and cause the advective movement of water and associated ions, including nutrients, from the surrounding water bodies (Rietkerk *et al.*, 2004; Cheng *et al.*, 2011). Increased nutrients and aerated soils in elevated zones are then expected to lead to greater plant productivity and enhanced potential for soil accretion (Eppinga *et al.*, 2008; Rietkerk and van de Koppel, 2008). As nutrients become concentrated in the more densely vegetated zones, productivity can decrease in the surrounding areas, and distinct vegetation patterns may form across the landscape (Rietkerk and van de Koppel, 2008).

Landscape patterning has been observed in wetlands worldwide, including the Okavango Delta and the Great Vasyugan Bog in Siberia (McCarthy *et al.*, 1993; Eppinga *et al.*, 2008). In these wetlands, elevated concentrations of nutrients and other dissolved ions have been detected in the

---

*Correspondence to: Pamela Sullivan, Southeastern Environmental Research Center, Florida International University, Miami FL, 33199, USA. E-mail: psull001@fiu.edu groundwater under isolated, wooded 'tree' islands. Groundwater under Okavango tree islands also has been shown to be supersaturated with respect to the minerals calcite and amorphous silica, and the precipitation of these minerals was associated with vertical soil accretion (McCarthy *et al.*, 1993). Woody plant transpiration also was associated with a water table depression and increased groundwater ion concentrations under eucalyptus plantations in the Pampas of Argentina (Engel *et al.*, 2005; Jobbágy and Jackson, 2007).

The Everglades is similar to those landscapes in that it consists of herbaceous freshwater marshes interspersed with isolated, tree-dominated communities that contain higher soil nutrient concentrations. These features comprise only approximately 2% of the land cover in the Everglades, but they represent important upland habitat for many vertebrates (Davis and Ogden, 1994). Since the 1940s, there has been a marked decline in tree island cover across the Everglades, and in the large Water Conservation Areas (WCA), between 60% (WCA 3) and 90% (WCA 2) of the tree island area has been lost (Patterson and Finck, 1999; Sklar and van der Valk, 2002). This period was also marked by the widespread loss of characteristic ridge-and-slough patterning and significant man-made changes in water levels in the Everglades (Ogden, 2005).

Although typically less than 1 m of elevation differences separates the surface of Everglades tree islands from the surrounding marsh soil surface, soil and pore-water phosphorus concentrations ([P]) are two to three orders of magnitude higher on the islands (Gann *et al.*, 2005; Ross *et al.*, 2006). The nitrogen-to-phosphorus (N:P), carbon-to-nitrogen (C:N), and ^{15}N:^{14}N ratios of leaves on these islands confirm localized nutrient accumulation (Wetzel *et al.*, 2005, 2011; Saha *et al.*, 2009, 2010; Wang *et al.*, 2010), although the mechanisms by which these nutrients accumulate have yet to be determined. Soil and pore-water [P] have been positively correlated with soil height above the surrounding marsh and negatively correlated to flood duration (Wetzel *et al.*, 2005; Ross *et al.*, 2006). Across the landscape, the highest soil [P] has been detected on tree islands in the southern Everglades (Wetzel *et al.*, 2009; Wang *et al.*, 2010; Ross and Sah, 2011). Nutrients on these islands are thought to originate from variable inputs of bird guano, bones, dry deposition, and transpiration-driven nutrient accumulation, although quantitative measures of these inputs have not been developed (Wetzel *et al.*, 2005; Coultas *et al.*, 2008).

Stable isotope studies by Saha *et al.* (2010) show that trees on Everglades islands rely on vadose zone soil moisture during the annual wet season to support transpiration and on deeper and lateral groundwater sources during dry periods. Several other studies have documented diurnal groundwater fluctuations and the dry season development of localized depressions in the water table beneath these tree islands (Ross *et al.*, 2006; Sullivan *et al.*, 2011; Wetzel *et al.*, 2011).

Recently, transpiration-driven ion accumulation has been suggested as a mechanism that may explain the petrocalcic horizons found in the soils beneath 20 large Everglades tree islands (Coultas *et al.*, 2008; Graf *et al.*, 2008). Ion exclusion during root water uptake and the subsequent mineral precipitation have been hypothesized to explain these enigmatic carbonate layers (Graf *et al.*, 2008; Schwadron, 2010; Chmura and Graf, 2011). Precipitation of carbonate soil layers may contribute to the differences in elevation between these islands and the surrounding marshes, although this has not been verified in field studies. What roles do transpiration and ion exclusion during root water uptake play in the accumulation and precipitation of dissolved solids in tree island soils? And if these processes are occurring, to what extent might their presence contribute to our understanding of the substrate composition, topographic profiles, and age of Everglades tree islands? Concurrent observations on tree island groundwater chemistry, transpiration, water and ion budgets, and geochemical modelling are needed to answer these questions.

The objective of this paper is to test three hypotheses: (1) transpiration-driven ion exclusion is concurrent with the influx of groundwater and influences the concentration of dissolved ions, including P, in tree island soils; (2) the magnitude of transpiration-driven ion accumulation differs along topographic gradients on tree islands; and (3) carbonate soil formation is supported by high ionic strengths (I) in tree island groundwater. To test these hypotheses, continuous sap flow, soil moisture, water level, and rainfall measurements were made for 3 years on a tree island in Everglades National Park (ENP). Sap flow, water levels, and soil moisture were used to identify and quantify groundwater uptake by overlying vegetation. Concentrations and ratios of dissolved ions as well as oxygen and hydrogen stable isotopes were used to determine the interaction between the tree island groundwater, marsh groundwater, and marsh surface water. Hydraulic head gradients, aquifer characteristics, and chloride concentrations were used to calculate the net ion transport between the tree island and the surrounding marsh. Lastly, groundwater saturation indices (SIs) were modelled with respect to aragonite, calcite, and hydroxyapatite (HYA) to examine potential soil-forming processes.

STUDY AREA

South Florida is subtropical with a 145-cm average annual precipitation (Duever *et al.*, 1994). The majority of rainfall occurs during the June-to-November wet season. Typically, potential evapotranspiration (ET) is greater than precipitation during the December-to-May dry season (German, 2000). The average annual temperature is 25 °C, with monthly means ranging from 15 to 32 °C (German and Sumner, 2002; Price *et al*., 2008).

Much of the freshwater Everglades is characterized by a parallel landscape patterning consisting of sawgrass (*Cladium jamaicense*) ridges separated by predominantly flooded sloughs and isolated tree islands (Ross *et al*., 2006; Larsen *et al*., 2007). Tree islands experience seasonal to no inundation during a given year. Surface water in the Everglades freshwater marshes is typically separated from the underlying limestone aquifer by a layer of peat with variable thicknesses and/or a layer of carbonate mud (less than 1 m, Ross and Sah, 2011). Where peat formations are thin or nonexistent, surface water is in direct contact with the underlying limestone aquifer.

Satinleaf Tree Island (25°39′34·85″N, 80°45′21·24″W) is located in Shark Slough (Figure 1), the principal drainage feature within ENP. Like many of the other islands in Shark Slough, Satinleaf is thought to have originated on a limestone outcrop or sediment mound (Loveless, 1959). The island is teardrop in shape, with a slightly elevated, upstream 'head' and an elongated, relatively low-elevation 'tail' oriented downstream. Satinleaf includes three woody community types distributed across an elevation and flooding gradient: hardwood hammock (HH), bayhead (BH), and BH swamp (BHS). The HH is located on the upstream end of the island at a ground elevation of 2·20 m (North American Vertical Datum of 1998, NAVD88) and is dominated by tropical hardwood species with minimal flooding tolerance. The BH, which surrounds the HH, is subject to wet season flooding and has a mean ground elevation of 1·60 m. The BHS, located at the downstream end of the tree island, is submerged for 5–9 months each year and has an average ground elevation of 1·45 m. The elevation of the surrounding marsh is 1·29 m. The HH community is dominated by tropical and subtropical tree species [e.g. *Eugenia axillaris* (EA), *Chrysophyllum oliviforme* (CO), *Bursera simaruba* (BS), and *Coccoloba diversifolia* (CD)], whereas the BH is dominated by subtropical and temperate tree species (e.g. *Annona glabra*, *Salix caroliniana*, *Morella cerifera*, and *Chrysobalanus icaco*). The canopy of HH has a leaf area index of 2·92 (Ruiz *et al*., 2011), similar to the BH canopy (Ross *et al*., 2006). Of the three communities, BHS has the

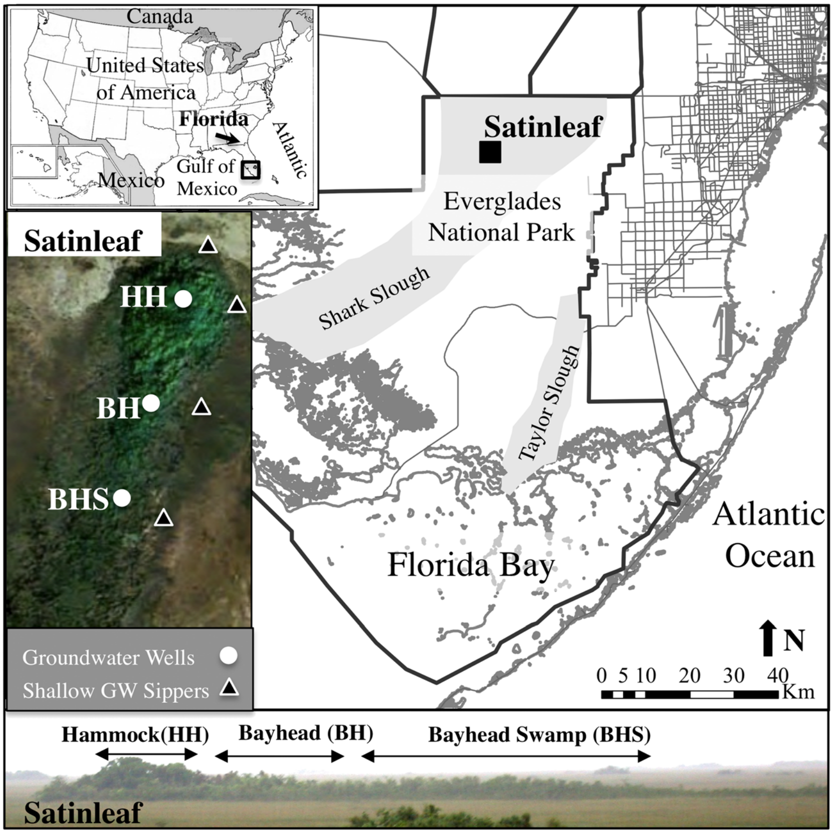

Figure 1. Satinleaf Tree Island in Everglades National Park, South Florida, United States. Groundwater wells (○) were monitored (left centre) in all three vegetation community types on the island: hammock (HH), bayhead (BH), and bayhead swamp (BHS) (bottom). Marsh groundwater was also monitored using shallow groundwater collectors (▲) (left centre).

lowest leaf area and is characterized by temperate tree species and a well-developed understory (Ross *et al.*, 2006).

METHODS

Precipitation, groundwater, surface water, and soil water monitoring

Total daily rainfall measurements during the 3-year study were obtained from a tipping-bucket gauge (G-620; http://sofia.usgs.gov/eden/index.php) located 1 km southwest of Satinleaf. Longer-term rainfall measurements during 25 years (1985–2010) were obtained from a gauge (S12D; http://my.sfwmd.gov/dbhydroplsql) located 14 km northeast of Satinleaf.

Shallow groundwater wells were installed near the centre of the HH, BH, and BHS communities, and a surface water monitoring station was installed in the nearby marsh (referred to as marsh surface water; Figure 1). All wells were 5·08 cm in diameter with an average depth of 67·7 cm, and they were installed in the sediment overlying the bedrock with similar elevations at the bottom of the wells (average of 95·3 cm; NAVD88). The top of each well and the surface water site were visually surveyed to the NAVD88 datum from nearby permanent benchmarks using a Nikon™ AS-2 34× automatic level and stadia rod. The total error in the water levels associated with the surveying technique, equipment, and water-level loggers was estimated as ±9·6 mm. Water levels at these sites were recorded every 30 min from April 2009 through September 2010 using HOBO™ U20 water-level loggers. Groundwater levels in the HH and marsh surface water also were monitored from July 2007 to June 2008 and from January to March 2009. Barometric pressure effects on water levels were corrected using a second HOBO™ U20 water-level logger located in a dry vented box on the HH. All water-level data were processed using HOBOware™. Between June 2008 and January 2009, marsh surface water levels were estimated by interpolating between surface water levels measured at two adjacent stations (NP202 and NP203, http://sofia.usgs.gov/eden/index.php) located ~4·8 km from the island.

Volumetric soil water content (VSWC) was measured using water content reflectometers (model CS615, Campbell Scientific Inc., Logan, UT) in the HH at depths of 10 and 30 cm every 15 min and averaged daily. Standard calibration coefficients were used to convert sensor signals to VSWC for soils that have an electrical conductivity of 1·8 dS m^{-1}.

Aquifer characteristics

Hydraulic conductivity. Sediment hydraulic conductivity was determined using slug tests in the HH, BH, and BHS wells. Water levels were monitored at 0·5-s intervals with an *in situ* Level Troll™ 500 pressure transducer for at least 3 min prior to the introduction or removal of 15- and 30-cm slugs. Water levels were then measured until they were within 5% of starting values. Sets (introduction and removal) of slug tests were repeated two to six times for both slug lengths. Water-level data were analysed assuming partially penetrating wells in an unconfined aquifer (Bouwer and Rice, 1976).

Specific yield. The available specific yield (S_{yr}) of tree island soils was measured in the vicinity of the wells in all three communities (Meyboom, 1967). Soil cores were collected using polycarbonate tubes with a diameter of 5·08 cm inserted into the ground to depth of refusal. The S_{yr} was determined separately on soil cores from the HH ($n = 4$; average length 7·0 cm), the BH ($n = 3$; average length 5·5 cm), and the BHS ($n = 2$; average length 10·5 cm). On average, 1 cm of compaction was observed when the core was removed. The cores were transferred intact to a laboratory where they were submerged slowly from the bottom in deionized water. Care was taken to ensure that cores were completely saturated, with no standing water at the top. The cores were allowed to drain for 12 h (Meyboom, 1967), and S_{yr} was determined according to Meinzer (1923; Table I). This process was repeated three times on each core, and all values were averaged to determine the S_{yr} of the soil per community type. S_{yr} values in deeper soil layers were not determined. Average surface S_{yr} values may underrepresent variability in specific yield with depth in the soil column.

Evapotranspirational losses from groundwater

Diurnal groundwater fluctuations from July 2007 through September 2010 were used to estimate groundwater withdrawals by phreatophytic vegetation (ET_{GW}) according to the expression developed by Hays (2003; Table I). Unlike the more commonly applied model for ET_{GW} developed by White (1932), the Hays method accounts for recharge during the drawdown period and allows for a more flexible rising period. The flexibility of the Hays method more accurately reflects the complexity of wetland hydrology (Mould *et al.*, 2010). Tidal forcing, pumping, or variations in atmospheric pressure were assumed to have a negligible effect on diurnal groundwater fluctuations. The ET_{GW} could not be calculated when surface water was present or during precipitation events. Total monthly ET_{GW} (cm m^{-1}) was calculated by multiplying the monthly average daily ET_{GW} by the number of days in that month.

Transpiration

From July 2007 through August 2010, sap flow velocity (v; mm s^{-1}) was monitored using Granier-type thermal

Table I. Description of equations and variables used to determine available specific yield, groundwater evapotranspiration, sap flow velocity, and groundwater fluxes on Satinleaf Tree Island.

Available specific yield (S_{yr}) $S_{yr} = \frac{V_{wd}}{V_{core}}$	(Meinzer, 1923; Meyboom, 1967) V_{wd} = volume of water drained (ml) V_{core} = total volume of the soil core (cm^3)
Groundwater evapotranspiration (ET_{GW}; mm day^{-1}) $ET_{GW} = \left[(H_1 - L) + \frac{(H_2 - L)}{T_1} T_2\right] 1000 S_y$	(Hays, 2003) H_1 and H_2 = high groundwater level at the beginning and end of the day, respectively (m) T_1 and T_2 = number of hours that occurred during the groundwater rising and drawdown periods, respectively (h) L = low water level (m) S_y = specific yield
Sap flow velocity (v; mm s^{-1}) $v = 0.119k^{1.231}$	(Granier, 1987; Clearwater *et al.*, 1999) k = temperature differences between the reference and heated thermal dissipation probes
Sapwood length ≥ 2 cm: $k = \frac{(\Delta T_m - \Delta T)}{\Delta T}$	ΔT_m = daily maximum temperature difference ΔT = measured daytime temperature difference
Sapwood length < 2 cm: $k = \frac{(\Delta T_m - \Delta T_{sw})}{\Delta T_{sw}}$	ΔT_{sw} = measured daytime temperature difference corrected for proportion of probe in nonconducting sapwood tissue
$\Delta T_{sw} = \frac{\Delta T - b\Delta T_m}{a}$	b = proportion in nonconducting sapwood tissue a = proportion of the probe in contact with conducting tissue
Ionic strength (I; mol kg^{-1}) $I = \frac{1}{2}\sum m_i z_i^2$	(Langmuir, 1997) m = concentration of ion i (mol kg^{-1}) z = charge of ion i i = ion
Groundwater flux per unit width of aquifer (Q; m^3 day^{-1}) $Q = K\frac{h_0^2 - h_l^2}{2L}$	K = hydraulic conductivity (m day^{-1}) h_0 and h_l = hydraulic heads of the surface water and groundwater, respectively (m) L = distance from the well to the marsh (m)

dissipation probes (model TDP-30™, Dynamax Inc., Houston, TX) installed in 10–12 trees comprised of four dominant species in the HH: EA (n = 3–5), CO (n = 2), BS (n = 3–4), and CD (n = 2). Sap flow measurements on CD were conducted between May 2009 and August 2010. Temperature differences (k) in the reference and heated TDP probes were recorded every 15 min on a data logger (model CR1000™ Campbell Scientific, Inc., Logan, UT), and hourly averages were used to calculate v (Grainer, 1987; Table I). If the sapwood length was less than 2 cm, the k values were corrected to account for the proportion of the probe in contact with the conducting tissue (Clearwater *et al.*, 1999; Table I).

The depth of active xylem in three individual trees of each of the four species (EA, CO, BS, and CL) was measured by injecting a 0·1% indigo carmine dye solution into each tree after removing a 5-mm core. After 2 h, a second 5-mm core was removed 2 cm above the injection point, and the length of the dyed core was measured. Approximately 60% of the sap flow probes had some contact with the nonconducting tissue. The length of three dyed cores was assumed to represent the sapwood radius of the tree and was used to solve for the sapwood area. Ten of the 12 trees cored to determine the sapwood area in 2010 were also monitored with sap flow probes. Linear regression was used to relate the sapwood area of the cored trees to diameter at breast height (DBH; R^2 = 0·85, p = 0·07, Figure 2). The DBH was measured on all trees in a 625-m^2 quadrat in the HH by Ross *et al.* (unpublished data) in November 2009. This quadrat represented approximately 91% of the total area of the HH community, and the species monitored for sap flow represented 83% of its total basal area. The total sapwood area and the sapwood area index (square metre of sapwood area per square metre of ground area) were calculated for three size classes (DBH < 6 cm, DBH = 6–12 cm, 12 cm > DBH) within each species found in the HH (Table II).

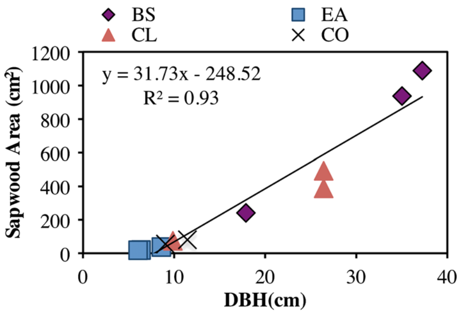

Figure 2. Linear regression derived between the sapwood area of cored trees [*Bursera simaruba* (BS), *Chrysophyllum oliviforme* (CO), *Coccoloba diversifolia* (CD), and *Eugenia axillaris* (EA)] and the diameter at breast height (DBH) to determine the sapwood area of all species in the stand.

The average daily sap flux velocity (V_{avg}) and sapwood area index (ρ) for $i = 4$ species in $j = 3$ size classes were used to estimate stand-level transpiration on a ground area basis, E (mm day^{-1}) after Engel *et al.* (2005):

$$E = \left(\sum_{j=1}^{3} \sum_{i=1}^{4} V_{\text{avg}.i,j} \rho i,j \right) \frac{\rho_{\text{Stand}}}{\rho_{\text{mon}}} \qquad (1)$$

The ratio of the total sapwood area of all the trees in the stand (ρ_{Stand}) to the total sapwood area of the species monitored for sap flow (ρ_{mon}) was used to scale the measurements to the whole-stand level. The value for this ratio was 1·2. Sap flow measurements on trees in the largest size class were made primarily on a single species (BS). Four BS trees in this size class were measured in 2007 and 2008. However, only one BS tree in this size class was successfully monitored during the period from January 2009 to August 2010 because of instrument failure. To improve our 2009–2010 estimates of E, a linear regression ($R^2 = 0{\cdot}61$; slope = 1·26; $p < 0{\cdot}01$) was developed between sap flow velocity measurements in this individual tree and the average sap flow velocity measured in three other BS trees in this size class during 2007–2008. The sap flow velocity for BS in this size class for 2009–2010 was then determined by multiplying the measurements in the single BS tree by the slope of this linear regression.

Groundwater and surface water chemistry

Discrete bimonthly samples of tree island groundwater and marsh surface water were collected from October 2008 to June 2010 for laboratory analysis. Each well was purged completely three times prior to sampling. Four groundwater samples from the marsh were collected at 3-month intervals between September 2009 and June 2010 using temporary shallow groundwater collectors (Fourqurean *et al.*, 1992) (Figure 1). Each collector, measured 80 cm in depth, was purged with helium to maintain an anoxic environment and sampled within 48 h of deployment.

Temperature and conductivity were measured *in situ* (YSI 85™, Yellow Springs, OH) along with pH (Orion Three-Star™ pH metre, Thermo Scientific Inc., Beverly, MD). Four samples were collected from all wells and surface water. Two of the samples were filtered using 0·45-µm glass fibre filters. One filtered sample and one unfiltered sample were preserved with 10% HCl to determine cation and total phosphorus ([TP]) concentrations, respectively. The other unfiltered sample was analysed for concentrations of total organic carbon ([TOC]). The remaining filtered sample was analysed for total alkalinity, major anions, phosphate concentration ([PO_4^{3-}]), and oxygen and hydrogen isotope analyses. One filtered water sample (0·45-µm glass fibre filter) and one acidified filtered water sample were taken from the shallow groundwater collectors and analysed for alkalinity and major anions, and cations, respectively. All samples were transported on ice to the lab where they were stored at 4 °C. [PO_4^{3-}], [TP], and [TOC] were analysed using an Alpkem™ 300 Series four-channel rapid-flow analyser, an Alpkem™ rapid-flow analyser with a two-channel expanded range detector, and a Shimadzu TOC-V™, respectively.

Stable isotopes of oxygen (δ^{18}O) and hydrogen (δD) in each water sample were determined using a Los Gatos DTL-100™ liquid-water isotope analyser and referenced to the Vienna Standard Mean Ocean Water. The analytical precision of the DTL was found to be ±0.1‰ and ±1.0‰ for oxygen and hydrogen, respectively. Total alkalinity calculated as milliequivalents per litre of bicarbonate [HCO_3^-] was determined by titration on all samples using

Table II. The sapwood area index for each species (*Bursera simaruba*, *Chrysophyllum oliviforme*, *Coccoloba diversifolia*, and *Eugenia axillaris*) within each size class (DBH < 6, 6–12, 12 cm < DBH) in the stand.

Species/size class	DBH < 6	6 < DBH < 12	DBH > 12
Bursera simaruba	1·93E−06	7·31E−05	3·41E−03
Chrysophyllum oliviforme	4·87E−06	1·54E−04	2·53E−04
Coccoloba diversifolia	0	1·23E−05	1·84E−05
Eugenia axillaris	4·56E−05	5·38E−05	0
Other	7·16E−06	8·89E−05	3·89E−04

DBH, diameter at breast height.

a Brinkman Titrino™ 751 titrator with a 0·1-M concentration of HCl to a pH of 2. The concentrations of the major cations (calcium [Ca^{2+}], magnesium [Mg^{2+}], sodium [Na^{+}], and potassium [K^{+}]) and anions (chloride [Cl^{-}] and sulfate [SO_4^{2-}]) were determined using a Dionex-120™ ion chromatograph. The charge balance of the major cations and anions for all of the water samples deviated from 0 by less than 10%. Major concentrations were then used to determine the overall ionic strength (I) of the water (Table I).

The mineral SIs for aragonite, calcite (both $CaCO_3$), and HYA ($Ca_{10}(PO_4)_3(OH)_2$) as well as the partial pressure of carbon dioxide (pCO_2) of each water sample were determined with the geochemical model PHREEQC (Parkhurst and Appelo, 1999). The chemical composition of each sample served as the input into PHREEQC. Positive SI values indicated that the water sample was supersaturated with respect to that mineral and signified potential precipitation. Negative SI values indicated undersaturated conditions with respect to that mineral and signified potential dissolution. SI values of 0 indicated equilibrium conditions, and neither precipitation nor dissolution was expected to predominate. SI values of $0{\cdot}00 \pm 0{\cdot}05$ for calcite and aragonite were considered to be at equilibrium.

Spearman correlations with $\alpha < 0{\cdot}05$ and $(r) > 0{\cdot}60$ between chemical constituents and SI values were considered significant. A one-way analysis of variance and a *post hoc* Tukey test ($\alpha = 0{\cdot}05$) were used to test the null hypothesis that HH, BH, and BHS groundwater chemistry was not significantly different.

Tree island hydrodynamics

Groundwater/surface water interactions were investigated by comparing the ionic ratios, [Cl^{-}], and $\delta^{18}O$ values sampled in each of the water bodies, and water bodies with similar chemical compositions indicated an increased interaction. The groundwater flux per unit width of aquifer (Q) on the island was also quantified (Table I). Positive fluxes indicated groundwater recharge (i.e. subsurface flow towards the island), whereas negative fluxes indicated groundwater discharge. Monthly averages of water inputs (Q, rainfall), losses (E), and changes in groundwater storage represented the primary components of the island water budget.

Changes in groundwater [Cl^{-}] represent a conservative tracer of surface water/groundwater interactions and overall water budgets, whereas changes in the groundwater concentration ratios of [Ca^{2+}]:[Cl^{-}] may indicate a disposal mechanism for chloride (e.g. downward fluxes) or sinks for Ca^{2+} (e.g. precipitation of $CaCO_3$). Monthly rainfall inputs and groundwater fluxes were multiplied by their average annual [Cl^{-}] and [Ca^{2+}]. Complete root exclusion of chloride was assumed in determining the effect of E on the Cl^{-} and Ca^{2+} budget. Rainfall [Cl^{-}] and [Ca^{2+}] values were obtained from the National Atmospheric Deposition Program (NADP) F11 Station (http://nadp.sws.uiuc.edu), located on Long Pine Key (ENP) from January 2009 through September 2010.

RESULTS

Rainfall and water levels

Total annual rainfall was similar to the 25-year average (128 cm year^{-1}) throughout the study except in 2009 (109 cm). Wet season monthly rainfall was below the 25-year average during the study period. Dry season (December to May) monthly rainfall was equivalent to or below the 25-year average except during 2009.

Marsh surface water and groundwater elevations in 2007–2010 varied seasonally from 0·81 to 2·05 m above NAVD88 (Figure 3A). Dry season groundwater levels in all treed communities were 2–5 cm lower than marsh surface water levels (Figure 3B). The largest differences between groundwater and surface water levels were detected during the 2008–2009 dry season. Wet season groundwater levels in all three communities were, within error, equivalent to the marsh surface water levels. Within the tree island, groundwater levels in the BH and BHS

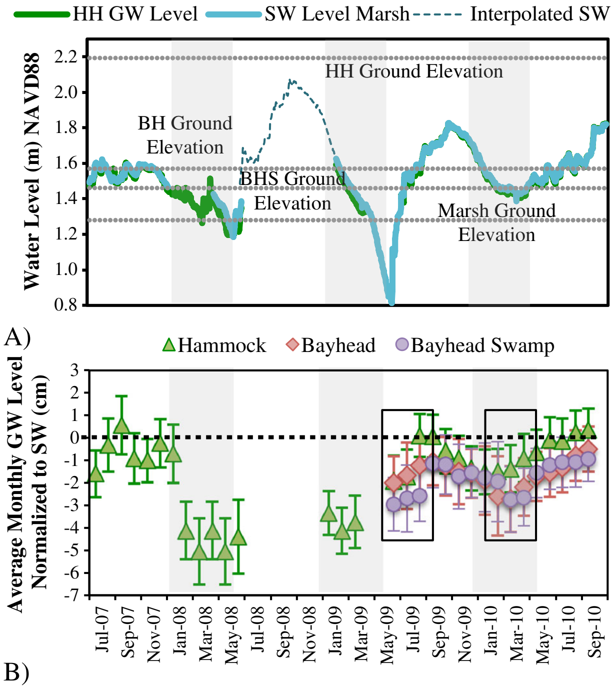

Figure 3. (A) Groundwater (GW) levels in the hardwood hammock (HH) community (black) and marsh surface water (SW) levels (grey) from July 2007 through September 2010. (B) Average monthly normalized GW levels in the HH (▲), bayhead (BH, ◆), and bayhead swamp (BHS, ●) communities. Positive values indicate that the GW was elevated compared with the SW, whereas negative values indicate GW levels were lower than SW levels. NAVD88, North American Vertical Datum of 1998.

were similar year-round and lower than those in the HH for approximately 30% of the study period.

Soil moisture and aquifer characteristics

Depth-averaged, monthly average VSWC ranged from 0·15 to 0·62 (θ, $cm^3\,cm^{-3}$, Figure 4). The lowest VSWC was concurrent with an extended period of below-average rainfall in the 2008–2009 dry season. Hydraulic conductivity and specific yield test results were similar across community types and averaged 4·01 m day^{-1} and 0·08 ± 0·05, respectively (Table III).

Stand-level transpiration (E) and groundwater evapotranspiration (ET_{GW})

Monthly average, total daily *E* in the HH ranged from 1·39 to 4·63 mm day^{-1} (Figure 4). Monthly average ET_{GW} was lower, ranging from 0·40 to 2·34 mm day^{-1} and, unlike *E*, exhibited a significant negative correlation to volumetric soil water content ($p < 0·01$, $R^2 = 0·49$). Groundwater uptake (ET_{GW}/E) by overlying phreatophytes was greatest when VSWC was low (Figure 5), which typically occurred in the dry season. The diurnal groundwater fluctuations used to calculate ET_{GW} were detected in the HH almost continuously throughout the study period (except in April–May 2009, when water levels dropped below the pressure transducer) but were detected only in the BH and BHS communities during the driest periods in 2009 (April–June) and 2010 (January–March). The average monthly ET_{GW} during these dry periods slightly differed between these communities with values of 1·37, 1·46, and 1·75 mm day^{-1} observed in the HH, BH, and BHS, respectively.

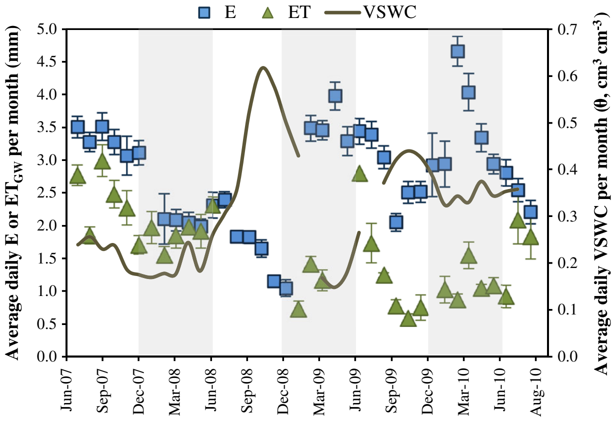

Figure 4. The average daily transpiration (*E*, 🟦) and groundwater evapotranspiration (ET_{GW}, ▲) per month and standard error for the hardwood hammock community compared with the average daily volumetric soil water content (VSWC, brown) per month.

Table III. The average hydraulic conductivity (*K*, m day^{-1}) and readily available specific yield (S_{yr}, unitless) and standard deviation of underlying geology of all three communities at Satinleaf (hardwood hammock, bayhead, and bayhead swamp).

Communities	*K* (m day^{-1})	S_{yr}
Hardwood hammock	3·46 ± 1·65	0·07 ± 0·03
Bayhead	6·23 ± 2·01	0·05 ± 0·02
Bayhead swamp	2·20 ± 0·40	0·08 ± 0·06

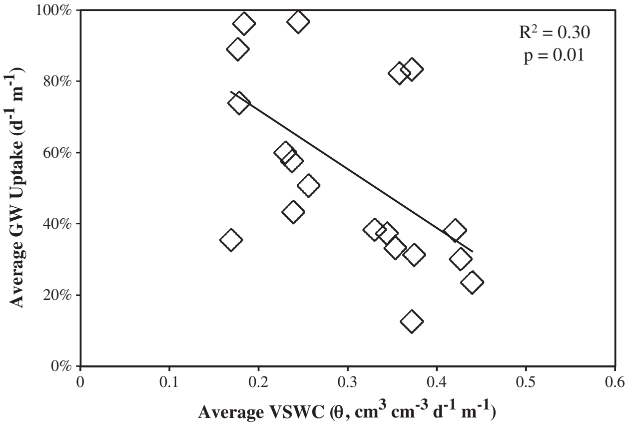

Figure 5. The correlation between the per cent of groundwater (GW) taken up by phreatophytes through transpiration and volumetric soil water content (VSWC, black).

Groundwater and surface water ion and stable isotope chemistry

Groundwater [HCO_3^-], [Cl^-], [Na^+], [Mg^{2+}], and [Ca^{2+}] in all three tree island communities were elevated compared with the concentrations of these ions in marsh surface water. Groundwater ionic strength (*I*) was highest in the BH and lowest in the HH (Table IV). Groundwater *I* in all three communities was highest in the wet season and lowest in the dry season and reflected seasonal changes in [Cl^-] (Figure 6A). The only exception occurred in March 2010 (a dry season month with above average rainfall) when relatively high [Cl^-] were detected in the HH and the BH. The seasonal variation in groundwater *I* was substantially dampened in the BHS compared with both the BH and HH. Marsh surface water *I* was highest during the dry season. The concentrations of all major ions, with the exception of sulfate [SO_4^{2-}] and ammonium [NH_4^+], in the tree island groundwater were positively correlated to each other (Table V). Concentrations of major ions in the marsh surface water were uncorrelated to [Ca^{2+}] or [HCO_3^-].

Surface water $\delta^{18}O$ values followed the same seasonal trends as dissolved ion concentrations (Figure 6B). During 2009, $\delta^{18}O$ values in the HH groundwater exhibited a dampened seasonal trend compared with those in the marsh surface water, whereas the $\delta^{18}O$ values during 2009 remained fairly constant in the BH and BHS. During 2010, the $\delta^{18}O$ values in groundwater at all locations were greater than those in surface water.

Table IV. The average values and standard error of temperature, conductivity, pH, major ions (HCO_3^-, Cl^-, SO_4^{2-}, Na^+, K^+, Mg^{2+}, and Ca^{2+}), nutrients (TP, PO_4^{3-}, and TOC), stable isotopes (δD and $\delta^{18}O$), ionic strength (I), SI values (aragonite, calcite, and hydroxyapatite) and pCO_2 in the groundwater in the HH, BH, and BHS and marsh surface water from October 2008 to June 2010.

Chemical constituents	Unit	Hammock	Bayhead	Bayhead Swamp	*p*	Surface water
Temperature	°C	24·4 ± 0·7	24·9 ± 0·9	25·0 ± 0·9	0·147	24·5 ± 1·7
Conductivity	$\mu s\,cm^{-1}$	958 ± 89 B, BS	1686 ± 55 H	1348 ± 58 H	<0·001	439 ± 43
pH	—	7·02 ± 0·04 B, BS	6·67 ± 0·09 H	6·69 ± 0·08 H	0·038	7·57 ± 0·12
HCO_3^-	$mmol\,l^{-1}$	6·23 ± 0·25 B, BS	12·35 ± 0·51 H, BS	10·28 ± 0·43 H, B	<0·001	3·18 ± 0·29
Cl^-	$mmol\,l^{-1}$	2·54 ± 0·17	5·36 ± 0·27 H, BS	3·96 ± 0·09 H, B	<0·002	0·89 ± 0·09
SO_4^{2-}	$mmol\,l^{-1}$	0·02 ± 0·07	0·08 ± 0·06	0·30 ± 0·10	0·11	0·11 ± 0·07
Na^{2+}	$mmol\,l^{-1}$	2·34 ± 0·13 B, BS	5·53 ± 0·22 H, BS	4·05 ± 0·08	<0·001	1·55 ± 0·12
NH_4^+	$mmol\,l^{-1}$	0·03 ± 0·01	0·06 ± 0·01	(u)		0·03 ± 0·02
K^+	$mmol\,l^{-1}$	0·06 ± 0·01	0·01 ± 0·01	(u)		0·10 ± 0·01
Mg^{2+}	$mmol\,l^{-1}$	0·47 ± 0·03 B, BS	0·94 ± 0·03 H, BS	0·79 ± 0·01 H, B	<0·001	0·40 ± 0·03
Ca^{2+}	$mmol\,l^{-1}$	2·70 ± 0·09 B, BS	5·66 ± 0·17 H, BS	4·79 ± 0·09 H, B	<0·001	1·23 ± 0·11
TP	$\mu mol\,l^{-1}$	16·49 ± 0·09 B, BS	1·33 ± 0·57 H	0·60 ± 0·11 H	<0·001	0·31 ± 0·09
PO_4^{3-}	$\mu mol\,l^{-1}$	1·87 ± 0·33 B, BS	0·27 ± 0·08 H	0·25 ± 0·18 H	<0·001	0·37 ± 0·29
TOC	$mmol\,l^{-1}$	1·27 ± 0·08 B, BS	4·64 ± 0·44 H	4·03 ± 0·33 H	<0·001	1·41 ± 0·10
δ^2H	‰	6·8 ± 1·1	4·3 ± 0·9	3·3 ± 0·6	0·075	7·9 ± 2·1
$\delta^{18}O$	‰	1·34 ± 0·29	0·82 ± 0·29	0·59 ± 0·21	0·114	1·08 ± 0·37
I	$mol\,kg^{-1}$	0·0122 ± 0·0006 B, BS	0·0243 ± 0·0005 H, BS	0·0209 ± 0·0003 H, B	<0·001	0·007 ± 0·001
$SI_{aragonite}$		−0·02 ± 0·06	0·24 ± 0·10	0·14 ± 0·09	0·1	0·11 ± 0·11
$SI_{calcite}$		0·12 ± 0·05	0·39 ± 0·10	0·28 ± 0·09	0·097	0·26 ± 0·12
SI_{HYA}		−1·68 ± 0·26 B, BS	−4·90 ± 0·49 H	−5·54 ± 0·62 H	<0·001	−2·47 ± 0·89
Log(pCO_2)	bar	−1·46 ± 0·04 B, BS	−0·93 0·08 H	−1·03 ± 0·08 H	<0·001	−2·45 ± 0·15

A one-way analysis of variance and a *post hoc* Tukey test were used to identify significant differences in the HH, BH, and BHS groundwater chemistry. (u) means under the detection limit. H, B, and BS indicated which communities groundwater chemistry significantly differed from the given communities HH, BH, and BHS, respectively, on the basis of the *post hoc* Turkey test (α = 0·05).
BH, bayhead; BHS, bayhead swamp; HH, hardwood hammock; SI, saturation index; TP, total phosphorus; TOC, total organic carbon.

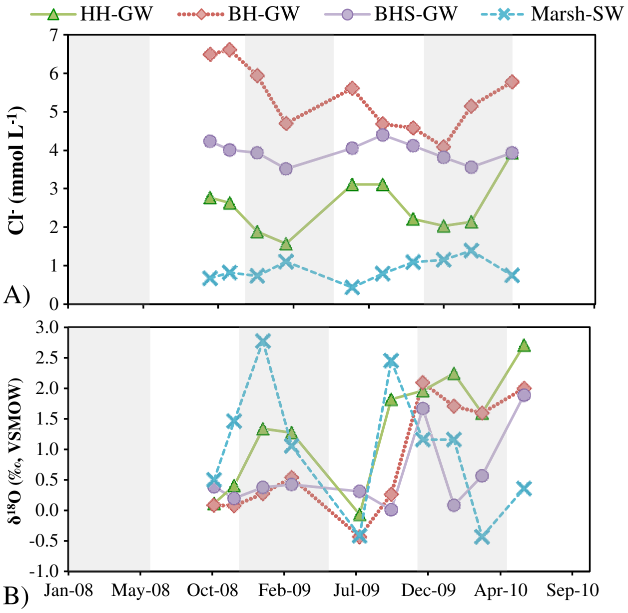

Figure 6. Chloride concentrations (A) and δ^{18}O values (B) in the marsh surface water (SW, ✕) and the groundwater (GW) in the hardwood hammock (HH, ▲), bayhead (BH, ◆), and bayhead swamp (BHS, ●) communities from October 2008 through June 2010. The dry seasons are indicated by the grey boxes. VSMOW, Vienna Standard Mean Ocean Water.

The BH and BHS groundwater consistently exhibited distinctly different stable isotope and geochemical signatures than marsh groundwater and surface water (Figure 7A). On the other hand, HH groundwater chemistry was indistinguishable from that of the marsh groundwater and surface water during the dry season and was similar to that of the BH and BHS communities during the wet season. The Na^{+}:Cl^{-} to Mg^{2+}:Ca^{2+} ratios in the HH, BH, and BHS wells were similar to each other but were different from the marsh surface water, whereas ratios in the marsh groundwater were between the marsh surface water and the tree island groundwater (Figures 7A and 7B).

Water, chloride, and calcium fluxes

Water budget calculations (Figure 8A) indicate that rainfall was the largest hydrologic input to Satinleaf during the annual wet seasons between 2007 and 2010. Estimates of groundwater flow along the hydraulic gradient between the marsh and the HH were greater than rainfall during the 2007–2010 dry season (Figure 8A). Wet season groundwater fluxes into HH approached 0. Groundwater discharge from the HH was observed occasionally (e.g. September 2007, February 2008, and May 2009). However, the largest loss of water from Satinleaf occurred by transpiration, which was highest during March and June.

The average [Cl^{-}] and [Ca^{2+}] in marsh surface water and groundwater (1·54 and 2·07 mmol l^{-1} and 1·24 and 3·67 mmol l^{-1}, respectively) were significantly greater than [Cl^{-}] and [Ca^{2+}] in rainfall (3·38 and 5·14 µmol l^{-1}; NADP-11 Long Pine Key). Estimates of groundwater Cl^{-} fluxes across the marsh/tree island boundary indicated an average input of 88·52 mmol m^{-3} per month to the tree island, whereas fluxes of [Ca^{2+}] were approximately twice that amount (162·07 mmol l^{-1}). Fluxes of both ions showed the same pattern with the greatest influx from Q estimated in the dry season when the lowest HH groundwater [Cl^{-}] and [Ca^{2+}] were detected (Figure 8B; only Cl^{-} shown). Average Cl^{-} and Ca^{2+} inputs to Satinleaf from rainfall were an order of magnitude smaller by comparison. Mass balance calculations indicated that the exclusion of Cl^{-} and Ca^{2+} during root water uptake could lead to an average increase of 208·82 and 221·67 mmol m^{-3} aquifer per month, respectively, beneath the HH. The average value of [Ca^{2+}]:[Cl^{-}] in HH groundwater samples (1·19) was 54% lower than the value of this ratio (1·83) in the marsh groundwater. This reduction suggests that the removal of Ca^{2+} from the solution occurs in the HH substrate, likely as a result of calcite precipitation.

Calcium carbonate geochemical modelling

The marsh surface water and groundwater in the BH and BHS had similar SI values and were predominantly at saturation or supersaturated with respect to aragonite and calcite (Table IV). The HH groundwater was typically undersaturated with respect to aragonite and saturated or supersaturated with respect to calcite. [Ca^{2+}] and [Cl^{-}] were positively correlated in the tree island groundwater when all of the communities were grouped together (Figure 9A). Groundwater SI_{calcite} and $SI_{\mathrm{aragonite}}$ values were positively correlated to [Ca^{2+}], [HCO_3^{-}], and [Mg^{2+}] beneath the tree island (Figure 9B; Table V) but not in the marsh surface water.

Modelled $p\mathrm{CO}_2$ in all tree island groundwater samples was elevated compared with $p\mathrm{CO}_2$ surface water estimates, and the highest values occurred in the BH and BHS (Table IV). Surface water $p\mathrm{CO}_2$ and groundwater I were both significantly correlated to $SI_{\mathrm{aragonite}}$ and SI_{calcite} and indicate that the saturation state of carbonate minerals in the surface water was driven by $p\mathrm{CO}_2$, whereas in the groundwater, I was the governing factor (Figure 9B and C; Table V).

Dissolved nutrients

Tree island groundwater [TOC], [TP], and [PO_4^{3-}] were enriched compared with those in the marsh surface water, with the highest [TP] and [PO_4^{3-}] found in the HH (Tables IV). When all three communities were grouped together to investigate whole tree island processes, groundwater [TOC] was negatively correlated to both [TP] and [PO_4^{3-}] but was positively correlated to most other major ion concentrations and to both SI_{calcite} and $SI_{\mathrm{aragonite}}$. SI_{HYA} values indicated that both the

Table V. Spearman correlation matrix of chemical constituents, ionic strength (I), and SI values of Satinleaf Tree Island groundwater ($n = 28$).

	Conductivity	pH	HCO_3^-	Cl^-	SO_4^{2-}	Na^+	NH_4^+	Mg^{2+}	Ca^{2+}	TP	PO_4^{3-}	TOC	δD	$\delta^{18}O$	I	$SI_{aragonite}$	$SI_{calcite}$	SI_{HYA}	$\log(pCO_2)$
Temperature	0·34	0·01	0·01	0·28	0·38	0·21	0·34	0·10	0·16	−0·33	−0·16	0·03	−0·07	0·00	0·16	0·25	0·28	−0·26	−0·02
Conductivity		−0·64	0·86	0·87	−0·16	0·87	0·40	0·88	0·87	−0·48	−0·57	0·79	−0·31	−0·15	0·88	0·53	0·52	−0·54	0·60
pH			−0·69	−0·71	−0·18	−0·73	−0·42	−0·68	−0·66	0·47	0·46	−0·46	0·55	0·39	−0·51	0·01	0·00	0·69	−0·95
HCO_3^-				0·84	−0·18	0·87	0·46	0·95	0·94	−0·42	−0·61	0·88	−0·31	−0·16	0·93	0·65	0·60	−0·46	0·72
Cl^-					0·03	0·97	0·38	0·91	0·92	−0·41	−0·49	0·72	−0·33	−0·26	0·95	0·55	0·54	−0·51	0·63
SO_4^{2-}						0·01	0·20	−0·10	−0·08	−0·37	−0·31	−0·27	−0·13	−0·11	−0·14	−0·07	−0·06	−0·37	0·05
Na^+							0·35	0·93	0·95	−0·45	−0·52	0·73	-·31	−0·30	0·96	0·58	0·56	−0·48	0·65
NH_4^+								0·45	0·43	−0·56	−0·67	0·48	0·25	0·46	0·30	0·41	0·42	−0·60	0·43
Mg^{2+}									0·99	−0·42	−0·60	0·86	−0·21	−0·16	0·98	0·69	0·66	−0·50	0·64
Ca^{2+}										−0·42	−0·60	0·85	−0·23	−0·20	0·99	0·70	0·67	0·49	0·62
TP											0·66	−0·33	0·27	0·02	−0·57	−0·25	−0·24	0·60	−0·46
PO_4^{3-}												−0·61	0·11	−0·07	−0·57	−0·47	−0·43	0·74	−0·51
TOC													−0·17	−0·04	0·83	0·70	0·67	−0·45	0·52
δD														0·74	−0·27	0·15	0·18	0·15	−0·50
$\delta^{18}O$															−0·25	0·16	0·17	0·04	−0·29
I																0·64	0·64	−0·523	0·64
$SI_{aragonite}$																	0·99	−0·20	0·09
$SI_{calcite}$																		−0·23	0·03
SI_{HYA}																			−0·56

SI, saturation index; TP, total phosphorus; TOC, total organic carbon.

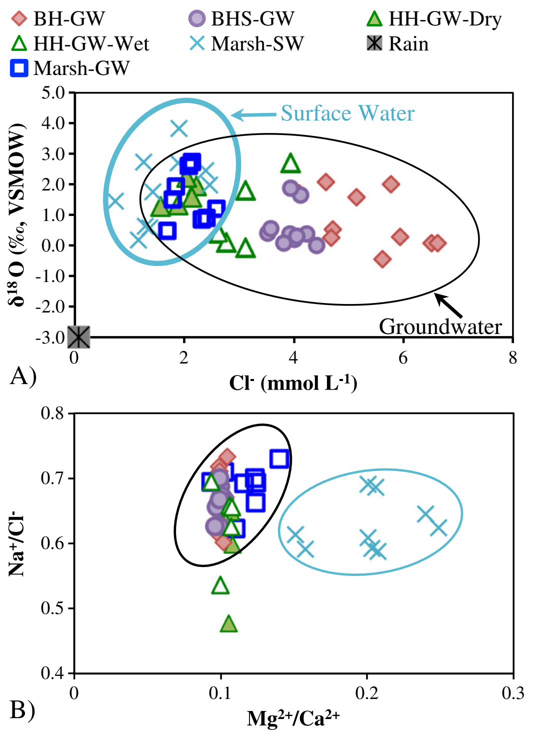

Figure 7. Chloride concentration compared with δ^{18}O values (A) and the ratio of Na^+ to Cl^- compared with Mg^{+2} to Ca^{+2} (B) for all groundwater (GW) and surface water (SW) sites. **δ^{18}O values of rainfall were taken from Price *et al.* (2008), whereas chloride values of rainfall came from the National Atmospheric Deposition Program (http://nadp.sws.uiuc.ed). BH, bayhead; BHS, bayhead swamp; HH, hardwood hammock; VSMOW, Vienna Standard Mean Ocean Water.

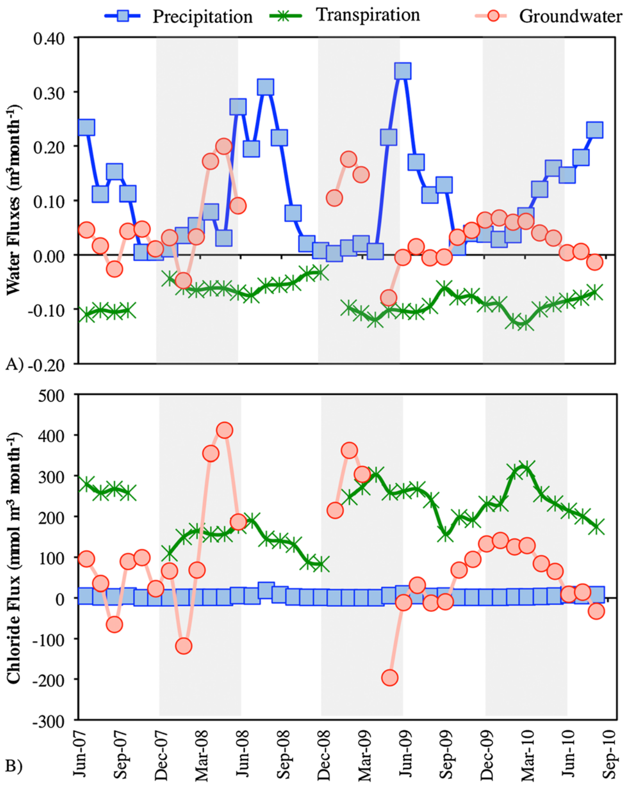

Figure 8. Fluxes of water (A) and chloride (B) in the hardwood hammock on Satinleaf as a result of precipitation inputs (■), inputs/losses of groundwater (●), and transpiration (*E*) (✳). Positive values represent inputs to the island, whereas negative values indicate that losses or outputs were negative.

groundwater and surface water were undersaturated with respect to HYA. When the communities were examined individually, a positive correlation between both [TP], [PO_4^{3-}], and [Cl^-], and [Na^+] was observed in the BH and BHS groundwater. Because ion exclusion during transpiration dominates the groundwater Cl budget, the positive correlation between [TP], [PO_4^{3-}], and [Cl^-] in the BH and BHS indicates that transpiration-driven groundwater inputs were the primary sources of P in these communities. On the other hand, in the HH groundwater, the negative correlation between [TP] and [TOC] indicated that the high groundwater [P] was likely derived from inorganic material, whereas the negative correlation between both [TP] and [PO_4^{3-}], and δ^{18}O values indicated that the high groundwater [P] was also related to the infiltration of ^{18}O-depleted rainwater (Figure 10A and B). PHREEQC modelling results indicated that HYA was more likely in the HH than in either the BH or the BHS. The nonlinear relationship between the groundwater SI_{HYA} and both SI_{calcite} and $SI_{\mathrm{aragonite}}$ in the HH community further indicated that the elevated groundwater SI_{HYA} was not a result of transpiration-driven root water uptake and ion exclusion, as was the case for groundwater SI_{calcite} and $SI_{\mathrm{aragonite}}$ values.

DISCUSSION

Wetzel *et al.* (2005) and Ross *et al.* (2006) were the first to hypothesize that root water uptake by phreatophytic vegetation on Everglades tree islands induces subsurface water flow from the surrounding marshes towards the island. These authors also suggested that there is a positive feedback mechanism whereby dissolved nutrients contained in the water flowing towards the island accumulate in the island soils, thereby supporting more dense vegetation, greater groundwater use, and increased nutrient transport and accumulation. The water balance calculations, hydrochemical and isotopic analyses, and geochemical modelling herein generally support this hypothesis. Moreover, the feedback mechanism exhibits significant spatial and temporal variability depending on seasonal rainfall patterns and the topographic position within an island.

Phreatophyte groundwater uptake and dissolved ion fluxes

The sap flow and groundwater measurements in the elevated HH community showed that the largest proportion of groundwater utilized during transpiration (ET_{GW}/E) was

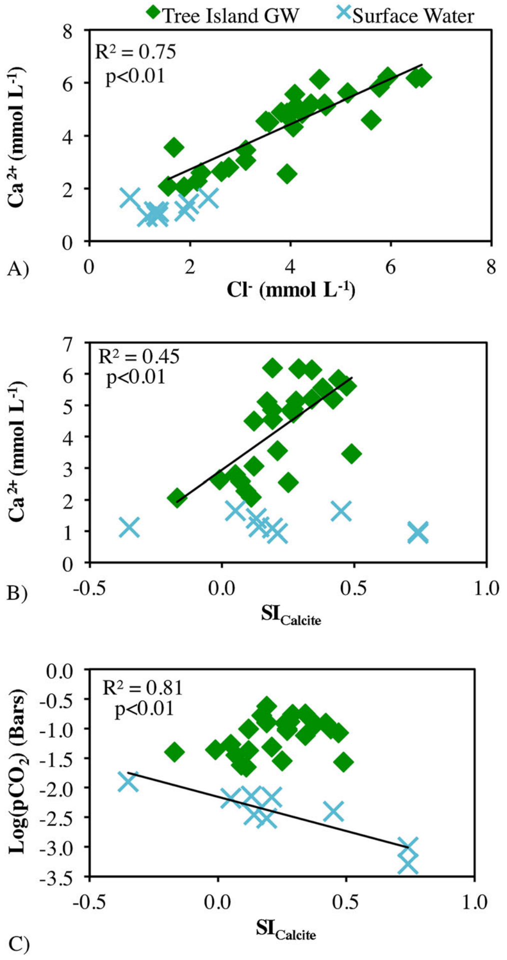

Figure 9. Correlations in tree island groundwater (GW, ◆) between the concentrations of calcium (Ca^{2+}) and chloride (Cl^-; A), the saturation indices of calcite ($SI_{calcite}$) and the concentration of calcium (B), and the calcite saturation indices and the partial pressure of CO_2 [$\log(pCO_2)$] in the surface water (SW, ×; C).

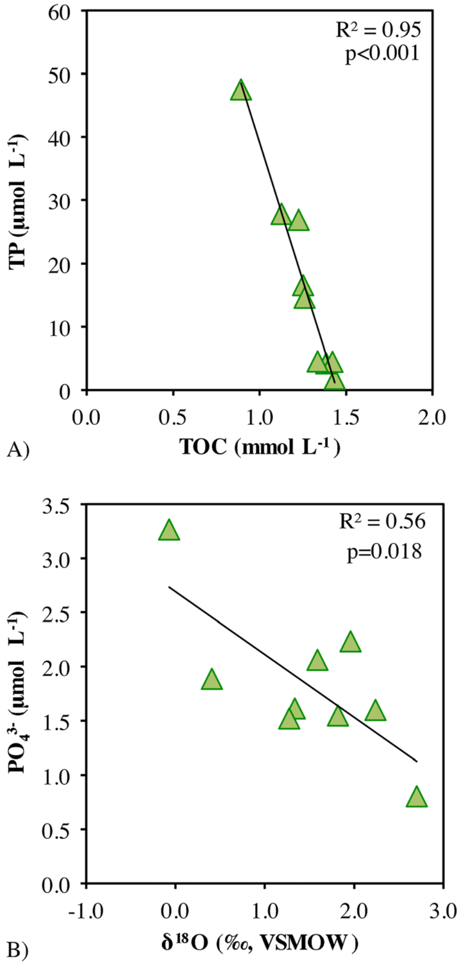

Figure 10. Correlations between total phosphorus (TP) and total organic carbon (TOC; A) and phosphate (PO_4^{3-}) and $\delta^{18}O$ values (B) in the hardwood hammock (▲) groundwater. VSMOW, Vienna Standard Mean Ocean Water.

concurrent with low volumetric soil water content values and the development of a dry season water table depression under the tree island. Average *E* values measured in the HH were similar to *E* reported from another hammock located in ENP (Villalobos-Vega, 2010). However, the mean monthly ET_{GW} rate (1·64 mm day^{-1}) recorded at Satinleaf was lower than the ET_{GW} reported by Villalobos-Vega (2010) and Sullivan *et al.* (2011) for constructed tree islands in the northern part of the Everglades. The lower ET_{GW} found at Satinleaf may be attributed, in part, to the use of the Hays instead of White method to calculate the ET_{GW}, as the latter only allows for recharge rates to be calculated between midnight and 0400 h, which potentially underestimates the recharge (Nichols, 1993).

The ET_{GW}/E in the HH at Satinleaf was similar to the ET_{GW}/E reported found by Ewe *et al.* (1999) and Saha *et al.* (2009) in other Everglades tree islands. By using the isotopic signatures of soil water, groundwater, and stem water, those studies concluded that the source of transpired water on the hammock portions of tree islands was approximately 80–90% groundwater during the dry season, compared with 30–50% during the wet season. The negative correlation found between ET_{GW} and volumetric soil water content on Satinleaf also confirms the results of Ewe *et al.* (1999) and Saha *et al.* (2009) and indicate that the trees on these islands act as facultative phreatophytes, which preferentially use soil moisture in the unsaturated root zone when it is available but which rely on deeper groundwater sources during periods of low rainfall. The Cl^-, Ca^{2+}, and water mass balance calculations confirm these results by indicating that inputs of groundwater adjacent to the island were a primary source of nearly all dissolved ions (with the exception of P) found in the tree island and that the seasonal increase in major ions could be explained as arising solely from ion exclusion during transpiration (i.e. root exclusion). These results generally supported hypothesis 1 and also indicated that transpiration-driven groundwater ion and nutrient fluxes to the island from surrounding areas were primarily a dry season phenomenon. During wet season months (e.g. August 2007), the hydraulic gradient between Satinleaf and the marsh indicated that groundwater sometimes discharged from the island. The discharge of nutrients from tree islands has been cited as a potential factor shaping nearby marsh plant species assemblages (Givnish *et al*., 2008).

The groundwater dynamics indicated by the hydraulic head gradients and E measurements were supported by the hydrochemical and isotopic data. For example, the similar δ^{18}O values and ionic ratios (e.g. Na^+:Cl^- and Mg^{2+}:Ca^{2+}) of the HH and marsh groundwater during the dry season indicated hydrologic connectivity and subsurface flow into the island. These ionic ratios in the marsh surface water were significantly different from the ratios found in HH groundwater, indicating that marsh surface water did not directly support E or recharge HH groundwater. During the wet seasons, the similar δ^{18}O values found in rainfall and the HH groundwater indicated that rainfall was the primary source of recharge in this community. However, groundwater I values were also highest during the wet season when they would normally be expected to decrease with the greater inputs of low ionic strength rainfall. For example, Wetzel *et al.* (2011) found that wet season groundwater I values were lower than dry season values beneath a peat-based island in an impounded area (WCA 3) to the north of ENP. The opposite relationship between rainfall and groundwater I at Satinleaf indicates the presence of additional mechanisms influencing tree island groundwater characteristics that have not been accounted for in previous studies.

Two primary mechanisms were hypothesized to explain the lower I in the HH groundwater during the dry versus wet seasons: (1) the dilution effect of the large, lateral inputs of low-I marsh groundwater to the tree island during the dry season, and (2) a separation between the depths at which ion exclusion during root water uptake occurs in the vadose zone and the depths to the groundwater table as measured in the piezometer. In mechanism (2), root water uptake occurs primarily in the groundwater table capillary fringe and unsaturated layers of the vadose zone, leading to an accumulation of ions above the water table that do not contribute to groundwater I. Schoups and Hopmans (2002) found that capillary forces resulting from transpiration in agricultural fields caused ions to accumulate at shallower depths in the vadose zone while depleting the concentration of major ions in underlying groundwater. A combination of large inputs of low-I marsh groundwater and a similar accumulation of dissolved ions in the vadose zone as shown by Schoups and Hopmans (2002) during periods of low groundwater tables at Satinleaf would explain both the low groundwater I values observed at the end of the dry season and, importantly, the subsequent increase in the groundwater I at the beginning of the wet season when rising water levels associated with increased rainfall solubilize the salts accumulated in the vadose zone during the preceding dry season. Recent shallow groundwater chloride modelling efforts on man-made tree islands in a large experimental facility in the Everglades support this hypothesis and further indicate the importance of vadose zone processes in the regulation of groundwater I (Sullivan *et al*., 2012) Additional measurements are needed to test this hypothesis and to better understand the significance of a seasonally fluctuating water table in regulating groundwater chemistry and carbonate precipitation in tree island soils.

Hydrochemical conditions across a topographic gradient

New findings from measurements in the lower-elevation BH and BHS communities have improved the current understanding of tree island and marsh surface water/groundwater interactions. ET_{GW} values in the BH and BHS equivalent to and possibly exceeding the HH were unexpected and indicated that the lower-elevation and more flood-tolerant BH and BHS communities were also reliant on groundwater during periods when water tables were beneath the surface. Hydraulic gradient measurements also indicated the potential for dry season advection of groundwater from the surrounding marshes into the BH and BHS. As was found for the HH, the ionic ratios and δ^{18}O values in the BH and BHS groundwater indicated little interaction with the surrounding surface water. Within the tree island, local hydraulic gradients between monitoring wells indicated that groundwater flowed from the HH into the BH and from the BH into the BHS, particularly at the beginning of the wet seasons. The flow of groundwater from higher-elevation to lower-elevation communities, combined with further ion exclusion during root water uptake, would explain the higher I values found in BH and BHS communities compared with that in the HH. Although the data support hypothesis 2, additional isotopic analyses of stem and source water combined with sap flow measurements will help define the phreatophyte-driven groundwater/surface water interactions across tree island topographic gradients and community types.

Transpiration-driven calcium carbonate formation

The geochemical modelling and water budget analyses indicate that the high groundwater I support the potential precipitation for calcite and aragonite in tree island soils. The SIs derived for these carbonate minerals indicated that precipitation could occur despite the observed high pCO_2 values, which would normally be associated with carbonate dissolution. Over time, calcium carbonate precipitation could contribute to soil formation and the topographic differences commonly observed between tree islands and the surrounding marshes. The source of spatial variation in SIs along the topographic gradient warrants further investigation because the data indicated calcite supersaturation in the HH, BH, and BHS communities, but aragonite undersaturation only in the HH community.

Dominant factors that control the saturation state of waters with respect to carbonate minerals include pCO_2, solubility of other carbonate minerals, temperature, ion exchange processes, and changes in I (Wigley and Plummer, 1976). The results of this study indicated that neither ion exchange reactions nor temperature controlled the saturation states of the tree island groundwater and marsh surface water, because the exchange of Na^+ or Mg^{2+} for Ca^{2+} was not observed in the ionic ratios and $SI_{\text{aragonite}}$ and SI_{calcite} values did not correlate to temperature (data not shown). Both $SI_{\text{aragonite}}$ and SI_{calcite} were positively and significantly correlated to pCO_2 in marsh surface water, indicating that pCO_2 controls the saturation state of carbonate minerals in the open marsh. However, calcite and aragonite supersaturation in the BH and BHS groundwater was a result of the extremely high $[Ca^{2+}]$ and I. The nearly one-to-one relationship between $[Ca^{2+}]$ and $[Cl^-]$ in the tree island groundwater indicates that the transpiration-driven accumulation of $[Cl^-]$ also drives groundwater $[Ca^{2+}]$ accumulation and, therefore, generally supports hypothesis 3 and indicates the potential precipitation of $CaCO_3$.

The concurrent aragonite undersaturation and calcite supersaturation in the HH groundwater is a result of the common ion effect. On Satinleaf, low-pH rainfall dissolves calcite and aragonite in the vadose zone as it comes to equilibrium with both minerals (Langmuir, 1997). Because aragonite has a higher solubility at any given pH (and pCO_2) compared with calcite, infiltrating water reaches equilibrium with calcite before aragonite. The continued dissolution of aragonite leads to an increase in $[Ca^{2+}]$ and $[HCO_3^-]$ in the water and the concomitant precipitation of calcite (Langmuir, 1997).

The calcite/aragonite data suggest that the petrocalcic soil horizon (Coultas *et al.*, 2008) found beneath the HH communities on many tree islands in the Everglades may be at least partially a result of the build-up of dissolved ions excluded during transpiration-driven root water uptake (Graf *et al.*, 2008). The formation of mineral soils on tree islands may also help mitigate soil loss due to oxidation and fire (Ross *et al.*, 2006), positively reinforcing their presence on the landscape. The formation of carbonate sediments could also play an important role in locally altering the underlying hydraulic properties of the tree islands sediments. Both at Satinleaf and on a tree island in the central Everglades, the aquifer hydraulic conductivities (1·01–43·20 m day^{-1}; Troxler and Childers, 2010) were greater than aquifer hydraulic conductivities reported for Everglades peat (0·56 m day^{-1}; Harvey *et al.*, 2000, 2004). The specific yield of tree island soils was slightly lower than that of Everglades peats, which typically range from 0·10 to 0·32, (Myers, 1999; Sullivan *et al.*, 2011). Further, soil cores as well as a detailed investigation of water table response to rainfall events at different stages across multiple islands are needed to understand the influence of carbonate precipitation on the hydraulic properties of the sediments.

Under climatic conditions similar to those in 2007–2010, the mass balance calculations suggest an annual average accumulation of 2·7 mol Ca^{2+} m^{-3} of HH substrate. Dividing the approximate total amount of substrate Ca^{2+} on a volumetric basis by this rate provides an estimate of the duration needed to accumulate this amount. A comparison of this estimate with an independent estimate of the period during which Everglades tree islands formed (2800–850 BP; Willard *et al.*, 2006) based on soil core dating provides a means to determine if transpiration-driven groundwater flux is sufficient to account for the total amount of substrate Ca^{2+}. An estimate of the time required to accumulate the total substrate Ca^{2+} via transpiration-driven processes that is less than the sediment-based estimate of Everglades tree island ages would suggest the presence of a co-occurring disposal mechanism (such as discharge of high-ionic-strength groundwater) that also regulates total Ca^{2+} accumulation.

Ross and Jones (2004) found that the HH surficial soils (0 to −20 cm below the surface) had an average bulk density of 0·5 g cm^{-3}, consisting of 25% carbonate and 30% organic matter. Assuming all the Ca^{2+} in the surface soil are associated with carbonate, the top 20 cm would contain approximately 250 mol Ca^{2+} m^{-2} of surface area. The bulk density of the petrocalcic soil layers found between −50 and around −100 cm on many tree islands in this part of the Everglades (Coultas *et al.*, 2008) is assumed to approximate the density values found for caliche layers in other systems, ranging between 1·4 and 1·9 g m^{-3} (Hennessy *et al.*, 1983). Assuming these layers are made entirely of $CaCO_3$, they therefore contain between 7000 and 9000 mol Ca^{2+} m^{-2}. Assigning an intermediate bulk density (1 g cm^{-3}) and a 50% carbonate composition for soil layers between −20 and −50 cm beneath the HH yields an additional 1500 mol Ca^{2+} m^{-2}. Under these assumptions, the HH substrate to −100 cm contains 8750–10 750 mol Ca^{2+} m^{-3}. At an accumulation rate of 2·7 mol year^{-1}, the total amount of time needed to accumulate this amount of Ca^{2+} is on the order of 3000–4000 years. This estimate is slightly greater than the upper limit of the estimated age of Everglades tree islands from Willard *et al.* (2006) and as such does not suggest the presence of a co-occurring disposal mechanism. However, given the large uncertainty in the estimates of the total amount of Ca^{2+} in the island soils, these calculations in and of themselves cannot be considered a reliable indicator of the presence or absence of a disposal mechanism. In tree islands of the Okavango delta, dense saline water that has accumulated in island soils because of ion exclusion during root water uptake periodically sinks into the underlying aquifer (Ramberg and Wolski, 2008). Density-driven removal of groundwater was not investigated as part of this study. However, the periodic flushing of high-ionic-strength groundwater during rainfall events when the direction of the subsurface hydraulic gradient results in groundwater discharge away from the island may function as a disposal mechanism regulating the accumulation of Ca^{2+} and other ions on Satinleaf. Investigations into the presence and potential magnitude of these types of disposal mechanisms will improve the understanding of the role of transpiration-driven groundwater flux in island formation and soil chemistry.

Groundwater phosphorus dynamics

The hydrochemical analyses indicate that although transpiration-driven groundwater fluxes are a source of dissolved nutrients and other ions found beneath all three tree island communities, the higher groundwater [TP] and $[PO_4^{3-}]$ observed in the HH community may originate from other sources. The negative relationships between the groundwater [P] and the SI_{calcite} and $SI_{\mathrm{argaonite}}$ values indicate that calcium carbonate dissolution is not a source of the high groundwater [P] in the HH. However, the inverse relationships found between [TOC] and both $[PO_4^{3-}]$ and [TP] in the HH groundwater do indicate a different inorganic origin. For example, during periods of low rainfall when local hydraulic gradients indicated groundwater flux from the marsh to the island, HH groundwater was characterized by relatively low I, $[PO_4^{3-}]$, and [TP] but was also undersaturated with respect to calcite, aragonite, and HYA. On the other hand, the data indicate that rainfall-driven percolation through the vadose zone resulted in elevated groundwater I, [TP], and $[PO_4^{3-}]$, which was concurrent with supersaturated and equilibrium conditions with respect to calcite and aragonite and near-equilibrium conditions with respect to HYA. These observations along with the groundwater SI_{HYA} indicate that P in the HH may originate from the dissolution of apatite located in the vadose zone. Recent mineralogical analyses using X-ray diffraction support this conclusion by showing that the soil [TP] in the most elevated portion of tree islands was also primarily derived from amorphous apatite (Bates *et al.*, 2010). Soil samples from the hammocks in the southern Everglades also showed a positive correlation between [TP] and noncarbonate minerals, which was attributed to the possible presence of HYA (Ross and Sah, 2011). Abundant buried bones and shells (Chmura and Graf, 2011) and deposits of bird guano (Wetzel *et al.*, 2005) on Everglades tree islands are potential sources of HYA.

CONCLUSIONS

Analyses of water-level, transpiration, and hydrogeochemical data presented herein generally support the hypothesis that root water uptake from phreatophytic vegetation drives groundwater fluxes from surrounding areas and P accumulation on Everglades tree islands. This process appears to dominate only during the dry seasons or during periods marked by low rainfall. The process represents the primary driver of soil and groundwater P accumulation only in the lower-elevation BH and BHS communities. In the highest-elevation HH community, the dissolution and weathering of P-containing inorganic minerals such as apatite from the vadose zone during the wet season appears to drive the observed high groundwater phosphorus concentrations. The supersaturation of carbonate minerals found in the BH and BHS groundwater caused by ion exclusion during root water uptake indicates for the first time that transpiration-driven processes may lead not only to P accumulation but also to potential mineral soil formation. This soil formation may, in turn, contribute to the localized topographic differences found between tree islands and the surrounding marshes. The present study indicates that transpiration in conjunction with other nutrient accumulation processes plays an important role in the maintenance of oligotrophic conditions and the landscape-scale patterning found in the Everglades. Future studies of water level, transpiration, and groundwater hydrogeochemistry will provide additional information regarding the potential effects of changing Everglades water management objectives on these biologically important systems.

ACKNOWLEDGEMENTS

Support for PLS for this project was provided by the Southeast Environmental Research Center (SERC) and Dissertation Year Fellowship at the Florida International University and the Everglades Foundation and developed in collaboration with the Florida Coastal Everglades Long-Term Ecological Research programme under the National Science Foundation and the NASA WaterSCAPES project. VE received support from the National Park Service, South Florida Natural Resources Center's Critical Ecosystem Studies Initiative. We thank the following individuals for their help in the field: Pablo Ruiz, Nate Colbert, Rafael

Traviso, Amartya Saha, Lawrence Lopez, Mike Kline, David Lagomasino, and Danielle Orgucak. Any use of trade, product, or firm names is for descriptive purposes only and does not imply endorsement by the US Government. This is SERC contribution no. 614.

REFERENCES

Bates AL, Orem WH, Newman S, Gawlik DE. 2010. Preliminary use of uric acid as a biomarker for wading birds on Everglades' tree islands. US Geological Survey Open File Report, Reston, VA.

Bouwer H, Rice RC. 1976. A slug test for determining hydraulic conductivity of unconfined aquifers with completely or partially penetrating wells. *Water Resources Research* **12**: 423–428. DOI: 10.1029/WR012i003p00423.

Cheng Y, Stieglitz M, Turk G, Engel V. 2011. Effects of anisotropy on pattern formation in wetland ecosystems. *Geophysical Research Letters* **42**: L0442. DOI: 10.1029/2010GL046091.

Chmura GL, Graf MT. 2011. The human trigger for development of tree islands in the Florida Everglades. American Geophysical Union (AGU)-Chapman Conference on Climates, Past Landscapes, and Civilizations, Santa Fe, NM, AGU Release No. 11–12, March 21.

Clearwater MJ, Meinzer FC, Andrade JL, Goldstein G, Holbrook NM. 1999. Potential errors in measurements of nonuniform sap flow using heat dissipation probes. *Tree Physiology* **19**: 681–687. DOI: 10.1093/treephys/19.10.681.

Coultas CL, Schwadron M, Galbraith JM. 2008. Petrocalcic horizon formation and prehistoric people's effect on Everglades tree island soils, Florida. *Soil Survey Horizon* **49**: 16–21.

Davis SM, Ogden JC. 1994. Everglades: The Ecosystem and Its Restoration. St. Lucie Press: Boca Raton, FL.

Duever MJ, Meeder JF, Meeder LC, McCollom JM. 1994. The climate in South Florida and its role in shaping the Everglades ecosystem. In Everglades: The Ecosystem and Its Restoration, Davis SM, Ogden JC (eds). St. Lucie Press: Delray Beach, FL; 225–248.

Engel V, Jobbágy EG, Stieglitz M, Williams M, Jackson RB. 2005. Hydrological consequences of *Eucalyptus* afforestation in Argentine Pampas. *Water Resources Research* **41**: W10409. DOI: 10.1029/2004wr003761.

Eppinga MB, Rietkerk M, Borren W, Lapshina ED, Bleuten W, Wassen MJ. 2008. Regular surface patterning of peatlands: confronting theory with field data. *Ecosystems* **11**: 520–536. DOI: 10.1007/s1-21-008-9138-z.

Ewe SML, Sternberg LO, Busch DE. 1999. Water-use patterns of woody species in pineland and hammock communities of South Florida. *Forest Ecology and Management* **118**: 139–148. DOI: 10.1016/S0378-1127(98)00493-9.

Fourqurean JW, Zieman JC, Powell GVN. 1992. Relationship between porewater nutrients and seagrasses in subtropical carbonate environment. *Marine Biology* **114**: 57–65. DOI: 10.1007/BF00350856.

Gann TT, Childers DL, Randeau DN. 2005. Ecosystem structure, nutrient dynamics, and hydrologic relationships in tree islands of the southern Everglades, Florida, USA. *Forest Ecology and Management* **214**: 11–27. DOI: 10.1016/j.foreco.2005.03.065.

German ER. 2000. Regional evaluation of evapotranspiration in the Everglades. US Geological Survey Water-Resources Investigations Report 00-4217, 48 pp.

German ER, Sumner DM. 2002. Evapotranspiration rates from two different sawgrass communities in South Florida during drought conditions. Second Federal Interagency Hydrologic Modeling Conference, Las Vegas, NV, 28 July–1 August, 12 pp.

Givnish TJ, Volin JC, Owen VD, Volin VC, Muss JD, Glaser PH. 2008. Vegetation differentiation in the patterned landscape of central Everglades: importance of local landscape drivers. *Global Ecology and Biogeography* **17**: 384–402.

Graf MT, Schwadron M, Stone PA, Ross M, Chmura GL. 2008. An enigmatic carbonate layer in Everglades tree island peats. *Eos* **89**; 117–119.

Granier A. 1987. Evaluation of transpiration in a Douglas-fir stand by means of sap flow measurements. *Tree Physiology* **3**: 309–320. DOI: 10.1093/treephys/3.4.309.

Harvey JW, Jackson JM, Mooney RW, Choi J. 2000. Interaction between groundwater and surface water in Taylor slough and vicinity, Everglades National Park, South Florida. US Geological Survey, Open File 00-483, Reston, VA.

Harvey JW, Krupa SL, Krest JM. 2004. Ground water recharge and discharge in the central Everglades. *Ground Water* **42**: 1090–1102. DOI: 10.1111/j.1745-6584.2004.tb02646.x.

Hays KB. 2003. Water use by saltcedar and associated vegetation on the Canadian, Colorado and Pecos Rivers in Texas. Dissertation, Texas A&M University.

Hennessy JJ, Gibbens RP, Tromble JM, Cardenas M. 1983. Water properties of caliche. *Journal of Range Management* **36**: 723–726.

Heuperman A. 1999. Hydraulic gradient reversal by tree in shallow water table areas and repercussions for the sustainability of tree-growing systems. *Agricultural Water Management* **39**: 153–167.

Jackson RB, Jobbágy EG, Nosetto MD. 2009. Ecohydrology bearing—invited commentary. Ecohydrology in a human-dominated landscape. *Ecohydrology* **2**: 383–389. DOI: 10.1002/eco.81.

Jobbágy EG, Jackson RB. 2007. Groundwater and soil chemical changes under phreatophytic tree plantations. *Journal of Geophysical Research* **112**: 1–15. DOI: 10.1029/2006JG000246.

Langmuir D. 1997. Aqueous Environmental Geochemistry. Princeton-Hall Inc.: Upper Saddle River, NJ.

Larsen LG, Harvey JW, Crimaldi JP. 2007. A delicate balance: ecohydrological feedbacks governing morphology in a lotic peatland. *Ecological Monographs* **77**: 591–614.

Loveless CM. 1959. A study of vegetation in the Florida Everglades. *Ecology* **40**: 1–9.

McCarthy TS, Ellery WN, Ellery K. 1993. Vegetation-induced, subsurface precipitation of carbonate as an aggradational process in permanent swamps of Okavango (delta) fan, Botswana. *Chemical Geology* **107**: 111–131. DOI: 10.1016/0009-2541(93)90105-R.

Meinzer OE. 1923. The occurrence of groundwater in the United States with a discussion of principles. US Geological Survey Water-Supply Paper 489.

Meyboom P. 1967. Groundwater studies in the Assiniboine River drainage basin: part II. Hydrologic characteristics of phreatophytic vegetation in south-central Saskatchewan. *Geologic Survey of Canada Bulletin* Vol. 1 139.

Mould DJ, Frahm E, Slzmann T, Miegel K, Acerman MC. 2010. Evaluating the use of diurnal groundwater fluctuations for estimating evapotranspiration in wetland environments: case studies in southeast England and northeast Germany. *Ecohydrology* **3**: 294–305. DOI: 10.1002/eco.108.

Myers RD. 1999. Hydraulic properties of south Florida wetlands peats. Dissertation, University of Florida.

Nichols WD. 1993. Estimating discharge of shallow groundwater by transpiration from greasewood in Northern Great Basin. *Water Resources Research* **29**: 2771–2778. DOI: 10.1029/93WR00930.

Ogden JC. 2005. Everglades ridge and slough conceptual ecological model. *Wetlands* **25**: 810–820.

Parkhurst PL, Appelo CAJ. 1999. User's guide to PHREEQC (version 2) – a computer program for speciation, batch-reaction, one-dimensional transport, and inverse geochemical calculations. US Geological Survey Water-Resources Investigations Report 99-4259, 738 pp.

Patterson K, Finck R. 1999. Tree Islands of the WCA 3A Aerial photointerpretation and trend analysis project summary report. Geonex Corporation, St. Petersburg, FL. Report to the South Florida Water Management District, West Palm Beach, FL

Price RM, Swart PK, Willoughby HE. 2008. Seasonal and spatial variations in the stable isotopic composition (δ^{18}O and δD) of precipitation in south Florida. *Journal of Hydrology* **358**: 193–205. DOI: 10.1016/j.jhydrol.2008.06.003.

Ramberg L, Wolski P. 2008. Growing islands and sinking solutes: processes maintaining the endorheic Okavango Delta as freshwater system. *Plant Ecology* **196**: 215–231. DOI:10.1007/sl1258-007-9346-1.

Rietkerk M, van de Koppel J. 2008. Regular pattern formation in real ecosystems. *Trends in Ecology & Evolution* **23**: 169–176. DOI: 10.1016/j.tree.2007.10.013.

Rietkerk M, Dekker SC, Wassen MJ, Verkroost AWM, Bierkens MFP. 2004. A putative mechanism for bog patterning. *The American Naturalist* **163**: 699–708.

Ross MS, Jones DT. 2004. Tree islands in the Shark Slough landscape: interactions of vegetation, hydrology and soils. Final report submitted to the Everglades National Park, Homestead, Florida, 1–196

Ross MS, Sah JP. 2011. Forest resource islands in a sub-tropical marsh: soil:site relationships in Everglades hardwood hammocks. *Ecosystems* **14**: 632–645. DOI: 10.1007/s10021-011-9433-y.

Ross MS, Mitchell-Brucker S, Sah JP, Stothoff S, Ruiz PL, Reed DL, Jayachandran K, Coultas CL. 2006. Interaction of hydrology and nutrient limitation in ridge and slough landscape of southern Florida. *Hydrobiologia* **569**: 37–59. DOI: 10.1007/s10750-006-0121-4.

Ruiz PL, Sah JP, Ross MS, Rodriguez D, Lambert AM. 2011. Monitoring of tree island conditions in the southern Everglades: the effects of hurricane and hydrology on the status and population dynamics of sixteen hardwood hammock tree islands. US Army Engineer Research and Development Center Cooperative Agreement: W912hz-09-2-0019.

Saha AK, Sternberg LO, Miralles-Wilhelm R. 2009. Linking water sources with foliar nutrient status in upland plant communities in Everglades National Park, USA. *Ecohydrology* **2**: 42–54. DOI: 10.1002/eco.38.

Saha AK, Sternberg LO, Ross MS, Miralles-Wilhelm R. 2010. Water source utilization and foliar nutrient status differ between upland and flooded plant communities in wetland tree islands. *Wetlands Ecological Management* **18**: 343–355. DOI: 10.1007/s11273-010-9175-1.

Schoups G, Hopmans JW. 2002. Analytical model for vadose zone solute transport with root water and solute uptake. *Vadose Zone Journal* **1**: 158–171.

Schwadron M. 2010. Prehistoric landscapes of complexity: archaic and woodland period shell works, shell rings and tree islands of the Everglades, south Florida. In Trend, Tradition, and Turmoil: What Happened to the Southeastern Archaic, Thomas DC, Sanger, MC (eds). *Anthropological Papers of the American Museum of Natural History* **93**: 113–146.

Sklar FH, van der Valk A. 2002. Tree islands of the Everglades: an overview. In Tree Islands of the Everglades, Sklar FH, van der Valk AG (eds). Kluwer Academic Publishers: Dordrecht, The Netherlands.

Sullivan PL, Price RM, Ross MS, Scinto LJ, Stoffella SL, Cline E, Dreschel TW, Sklar FH. 2011. Hydrologic processes on tree islands in the Everglades (Florida, USA): tracking the effects of tree establishment and growth. *Hydrogeology Journal* **19**: 367–378. DOI: 10.1007/s10040-010-0691-0.

Sullivan PL, Price RM, Miralles-Wihelm F, Ross MS, Scinto LJ, Dreschel TW, Sklar F, Cline E. 2012. The role of recharge and evapotranspiration as hydraulic drivers of ion concentrations in shallow groundwater on Everglades tree islands, Florida (USA). *Hydrological Processes*. Online. DOI: 10.1002/hpy.9575

Troxler TG, Childers DL. 2010. Biogeochemical contributions of tree islands to Everglades wetland landscape nitrogen cycling during seasonal inundation. *Ecosystems* **13**: 75–89. DOI: 10.1007/s10021-009-9302-0

Villalobos-Vega RM. 2010. Water table and nutrient dynamics in neotropical savannas and wetland ecosystems. Dissertation, University of Miami.

Wang X, Sternberg LO, Ross MS, Engel VC. 2010. Linking water use and nutrient accumulation in tree islands upland hammock plant communities in the Everglades National Park, USA. *Biogeochemistry* **104**: 133–146. DOI: 10.1007/s105333-10-9492-8.

Wetzel PR, van der Valk AG, Newman S, Gawlik DE, Gann TT, Coronado-Moliana CA, Childers DL, Sklar FH. 2005. Maintaining tree islands in the Florida Everglades: nutrient redistribution is the key. *Frontiers in Ecology and the Environment* **3**: 370–376. DOI: 10.1890/1540-9295(2005)003.

Wetzel PR, van der Valk AG, Newman S, Coronado CA, Troxler TG, Childers DL, Orem WH, Sklar FH. 2009. Heterogeneity of phosphorus distribution in a patterned landscape, Florida Everglades. *Plant Ecology* **200**: 83–90. DOI: 10.1007/s11258-008-9449-3.

Wetzel PR, Sklar FH, Coronado CA, Troxler TG, Krupa SL, Sullivan PL, Ewe S, Price RM, Newman S, Orem WH. 2011. Biogeochemical processes on tree islands in the Greater Everglades: initiating a new paradigm. *Critical Reviews in Environmental Science and Technology* **41**: 670–701. DOI: 10.1080/10643389.2010.530908.

White WN. 1932. A method of estimating ground-water supplies based on discharge by plants and evaporations from soils: results of investigations in Escalante Valley, Utah. US Geological Survey Water-Supply Paper, 659-A.

Wigley TML, Plummer LN. 1976. Mixing of carbonate waters. *Geochimica et Cosmochimica Acta* **40**: 989–995. DOI: 10.1016/0016-7037(76)90041-7.

Willard DA, Bernhardt CE, Holmes CW, Landacre B, Marot M. 2006. Response if Everglades tree islands to environmental change. *Ecological Monographs* **76**: 565–583.